Stoichiometry-Controlled Fabrication of CuxS Hollow Structures With Cu2O as Sacrificial Templates

ARTICLE *in* CRYSTAL GROWTH & DESIGN · JULY 2011

Impact Factor: 4.89 · DOI: 10.1021/cg101283w

4 AUTHORS, INCLUDING:

Yang Shang
Beihang University(BUAA)
10 PUBLICATIONS **105** CITATIONS

SEE PROFILE

CRYSTAL GROWTH & DESIGN

ARTICLE

pubs.acs.org/crystal

Stoichiometry-Controlled Fabrication of Cu_xS Hollow Structures With Cu_2O as Sacrificial Templates

Dong-Feng Zhang, Hua Zhang, Yang Shang, and Lin Guo*

School of Chemistry and Environment, Beihang University, Beijing 100191, China

Supporting Information

ABSTRACT: In this work, we report the successful composition-controlled synthesis of copper sulfides hollow structures using Cu_2O nanocrystals as sacrificial templates via a Kirkendall-based process. The direct introduction of S^{2-} glycol solution into the Cu_2O-containing mother solution produced Cu_7S_4 nanocrystals, while CuS formed with Cu_2O experienced a separation and drying process as sacrificial templates. Fourier transform infrared (FTIR) and X-ray photoelectron spectroscopy (XPS) data reveal that a layer of CuO existed on the surface of the dried Cu_2O. We believe the surface states of Cu_2O templates played key roles in the stoichiometry control. The presence of CuO catalyzed the oxidation from Cu^+ to Cu^{2+}. The type of sulfur source is importance for the formation of hollow structures. The UV−vis−NIR absorption investigation demonstrates a significant quantum confinement effect and stoichiometry-dependent features. It may provide a new approach for the stoichiometry-controlled synthesis of chalcogenides and would aid a better understanding of the optical behaviors of copper sulfides.

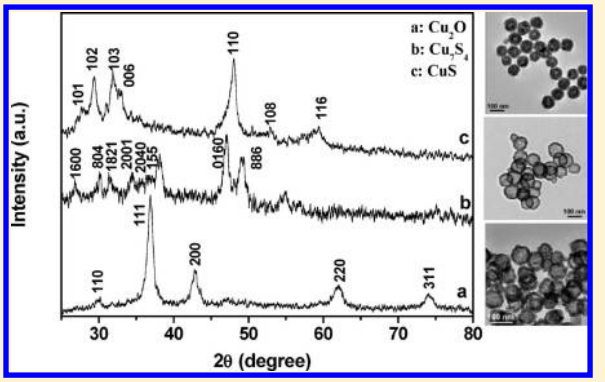

INTRODUCTION

Transition-metal chalcogenides represent an important member in the family of semiconductors owing to their excellent properties and potential applications. Among them, copper sulfides (Cu_xS) attract considerable research interest with rich stoichiometries as an important character. At least five stable phases exist at room temperature, including covellite (CuS), anilite($Cu_{1.75}S$), digenite ($Cu_{1.8}S$), djurlite ($Cu_{1.95}S$), and chalcocite (Cu_2S). The varied structures and valence states are expected to produce unique optical and electrical properties. It was evidenced that the resistance response to gas has a close relationship with the stoichiometry and morphology of $Cu_{2-x}S$.[1,2] The optical band gaps were found to be dependent on the x value of the Cu_xS, although some controversial conclusions were drawn.[3−6] For example, a blue shift in the band gap was observed with the increase of the copper deficiency in most reports (E_g = 1.2 eV for Cu_2S, 1.5 eV for $Cu_{1.8}S$, and 2.0 eV for CuS),[3−5] while Sharma et al. reported a contrary result (E_g = 1.26 eV for CuS, 1.96 eV for $Cu_{1.4}S$, and 2.31 eV for Cu_2S).[6]

Stimulated by their rich properties and promising application potential, great efforts were devoted to the fabrication of Cu_xS nanostructures. Copper sulfides with various morphologies including nanorods,[7] nanotubes,[8] nanoflakes,[9] nanowalls,[10] nanotrees,[11] nanocages,[12] and hollow spheres[13] were synthesized by employing various synthesis strategies. For example, by decomposing a sulfur-containing copper(II) complex, $Cu(S_2CNEt_2)_2$, spherical $Cu_{1.8}S$ (digenite) nanocrystals were synthesized in a high boiling point coordinating solvent.[14] CuS hollow spheres were produced by taking advantage of an oil/water interface with CS_2 as the sustained-release sulfur resource in the cyclohexane/water/Triton X-100 micelle system.[15] Cu_7S_4 hollow structures were converted from regular-shaped Cu_2O or $Cu(OH)_2$ nanocrystals as sacrificial templates.[16]

Most of the works focused on the morphology control, and the experiments were carried out under different conditions. The different size, shape, and surface states of the products result in inconsistent data, which greatly limits the understanding of the stoichiometry-dependent properties. Systematic composition control is an efficient strategy to address the existing uncertainty about the properties of copper sulfides. However, it is still a great challenge for the composition-controlled synthesis. Only a few reports were concerned this issue because of the lack of efficient fabrication methods. Xu et al. reported the composition variation from $Cu_{1.75}S$ to Cu_2S by changing the reaction atmosphere from air to nitrogen during the fabrication of $Cu_{2-x}S$ mesocages based on the Kirkendall effect.[17] Very recently, Burda and Zhu et al. synthesized $Cu_{2-x}S$ (x = 1, 0.2, 0.03) nanocrystals via three different chemical methods to investigate the size- and composition-dependent optical properties.[18] In this paper, we report that the composition control of copper sulfides can be achieved by simply adjusting the post-treatment procedure of the Cu_2O templates through a Kirkendall-based process. The presence of CuO covered on the outside of Cu_2O by partial oxidation is believed to catalyze the transformation from Cu^+ to Cu^{2+}.

Received: September 30, 2010
Revised: June 2, 2011
Published: July 22, 2011

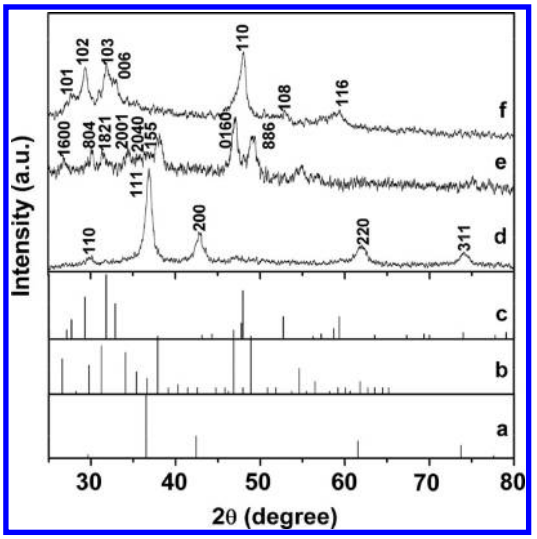

Figure 1. Standard XRD patterns of (a) Cu_2O with JCPDS No. 77-0199, (b) Cu_7S_4 with JCPDS No. 23-0958, (c) CuS with JCPDS No. 06-0464. Patterns d−f are the corresponding XRD patterns of Cu_2O spherical nanotemplates, Cu_7S_4, and CuS hollow nanospheres, respectively.

The as-prepared Cu_7S_4 and CuS nanocrystals exhibit remarkable quantum size effects and carrier concentration dependent plasmonic absorption.

EXPERIMENTAL SECTION

Synthesis. All of the chemical reagents used were of analytical grade and used without further purification. Hollow spheres of copper sulfides with different stoichiometries were fabricated by a Cu_2O-templated sulfidation process. In a typical procedure for the synthesis of Cu_2O templates, 0.001 mol of $CuAc_2 \cdot H_2O$ and 0.01 mol of polyvinylpyrrolidone (PVP, MW 30 000) were dissolved in 30.0 mL of glycol under intensive stirring for 2 h. A homogeneous transparent light green solution was obtained. Then, 10.0 mL of NaOH (2.0 mol·L^{-1}) was added dropwise into the above solution. The solution gradually turned blue, indicating the formation of copper hydrate. After stirring of the solution for 0.5 h, 10.0 mL of ascorbic acid (Vc) solution (0.3 mol·L^{-1}) was introduced. The mixture was kept at 55 °C for 30 min. A turbid yellow suspension was produced, indicating the formation of Cu_2O as confirmed by X-ray diffraction (XRD) characterization (Figure 1d).

For the synthesis of Cu_4S_7 nanocrystals, 20.0 mL of Na_2S EG solution (0.15 mol·L^{-1}) was directly added into the turbid suspension and the reaction was kept at 55 °C for 1 h. The resulting dark precipitate (denoted as sample A) was collected by centrifugation and decanting, followed by washing with distilled water 3 times and absolute ethanol 2 times to remove the residual polymer and inorganic ions, and finally dried in a vacuum at 50 °C for 5 h for further characterizations.

For the synthesis of CuS nanocrystals, the Cu_2O nanocrystals were first separated from the suspension by centrifugation and decanting. After thorough washing, it was dried at 50 °C for 5 h. The average weight of the as-prepared Cu_2O nanocrystals was measured as about 0.030 g. Assuming the weight loss is 0.005 g during the washing, the concentration of the Cu_2O nanoparticles for the fabrication of Cu_4S_7 can be calculated as about 0.5 g/L. Therefore, we take 0.5 g/L as the constant concentration of Cu_2O templates. Then, 0.030 g of Cu_2O nanocrystals was dispersed into 40.0 mL of glycol to make its concentration equal to that in group one. 20.0 mL of Na_2S (0.15 mol·L^{-1}) glycol solution was added into the dispersion and heated at 55 °C for 1 h. The deposited black precipitate (denoted as sample B) was collected according to a process identical to those for the sample A.

Instruments. An X-ray powder diffraction pattern was recorded on a powder sample with Rigaku, D/max-2200 diffractometer employing Cu Kα radiation ((λCu Kα_1 = 1.54056 Å) at a scanning rate of 0.02° s^{-1} ranging from 30 to 80°. Scanning electron microscopy (SEM) observations were carried out with a Hitachi-S4300 operated at an acceleration voltage of 20 kV. Transmission electron microscopy (TEM) and high-resolution TEM (HRTEM) characterizations were performed with JEOL JEM-2100F operated at 200 kV. Absorption spectra were recorded on a SolidSpec-3700 UV−vis−NIR spectrophotometer made in Shimadzu, Japan. Fourier transform infrared (FTIR) spectra were recorded on Nicolet AVATAR360 FTIR spectrophotometer. X-ray photoelectron spectroscopy (XPS) measurements were carried out on an Axis Ultra spectrometer at a pressure lower than 10^{-8} Torr with a standard Al Ka excitation source (1486.6 eV). The charging effect was corrected by adjusting the binding energy of the main C 1s peak to 284.6 eV.

RESULTS AND DISCUSSION

XRD characterization revealed that the yellow precipitate is cuprite Cu_2O with JCPDS No. 77-0199 (Figure 1a). No peaks from impurities such as CuO and Cu can be identified. Figure 1, panels e and f are the corresponding XRD patterns of samples A and B, respectively. All the peaks in Figure 1b can be indexed to the monoclinic Cu_7S_4 (JCPDS No. 23-0958) with the $C2/m$ space group, while the diffractions in Figure 1f match well with Bragg reflections of the hexagonal CuS with JCPDS No. 06-0464. XRD characterizations demonstrate that composition control was achieved for the copper sulfide nanocrystals.

TEM observations reveal that the Cu_2O templates were hollow spherical structures with diameters of ca. 90 nm and an interior space of ca. 30 nm (Figure 2a). The template effect of PVP is believed to be responsible for the Cu_2O to form a hollow structure on the basis of our previous works.[19] No obvious morphology changes were observed for the untreated and separated-dried Cu_2O nanocrystals. After sulfidation, the products remained hollow spherical structures as shown in Figure 2b,c. However, the inner void space was greatly enlarged, which produced a much thinner shell (ca. 8 nm) of copper sulfides than that of Cu_2O templates. The corresponding broad view SEM images are shown in Supporting Information Figure S1.

HRTEM was employed to get the detailed structure information of the products. Figure 3b is a typical HRTEM image recorded from the edge of a single Cu_7S_4 hollow nanosphere (framed area in Figure 3a). The spacing between two adjacent lattice fringes is 0.29 nm, agreeing with that of the (1821) planes of Cu_7S_4. There is no specific orientation relationship found among the grains. In the HRTEM image (Figure 3d) of a CuS hollow nanosphere (Figure 3c), several sets of fringes were identified. The fringe with an interplanar spacing of 0.19 nm corresponds to the (110) plane of hexagonal CuS, while the 0.28 and 0.30 nm spacing is coincident with the (103) and (102) planes of CuS, respectively. The coexistence of different sets of fringes in one HRTEM image is a typical feature of polycrystalline. HRTEM results agree well with the XRD characterizations, which further confirm the successful stoichiometry control of Cu_xS. The insets in Figure 3a,c are the corresponding selected area electron diffractions (SAED) patterns. The diffraction rings confirm their polycrystalline structures. Besides the diffractions from targeted cupper sulfides (such as Cu_7S_4 in Figure 3a and

dx.doi.org/10.1021/cg101283w |*Cryst. Growth Des.* 2011, 11, 3748–3753

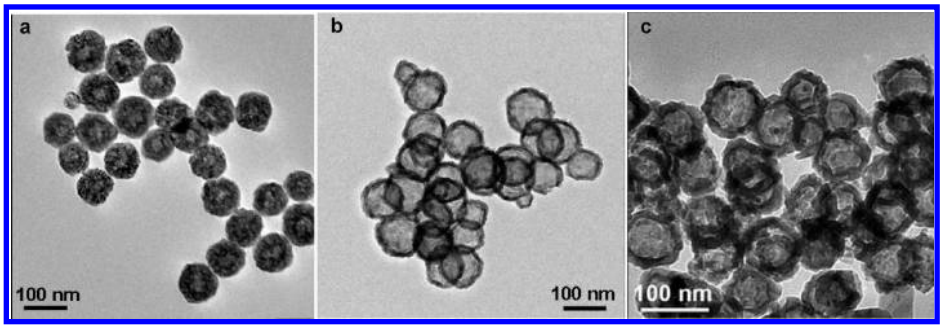

Figure 2. TEM images of (a) Cu_2O spherical nanotemplates, (b) Cu_7S_4, (c) CuS hollow nanospheres.

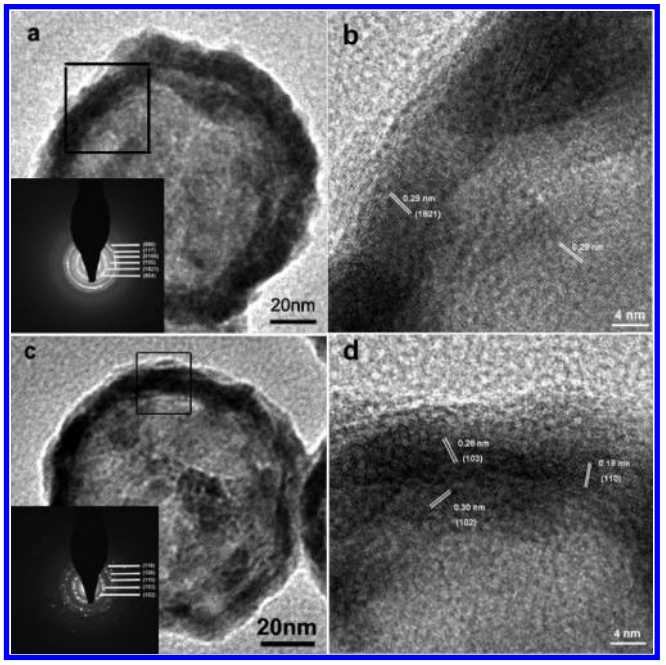

Figure 3. (a, c) High-magnification TEM images, and (b, d) the corresponding HRTEM images of individual Cu_7S_4 and CuS hollow spheres, respectively.

CuS Figure 3c), no unindexed rings were observed in both cases, which indicates the high phase purity of the products.

Previously, we reported the shape-controlled fabrication of Cu_2O polyhedrons.[20] By performing similar procedures with these polyhedrons as templates, we found in situ transformation and composition control are also possible. Figure S3, Supporting Information gives the examples with octahedrons as templates. It can be seen that the sulfides maintained the shape of octahedrons except for the hollow interiors. XRD results verified the composition control definitely.

Further experiments reveal that the sulfur sources played important roles in the formation of hollow structured sulfides. For comparison, thioacetamide and thiourea were also used as a sulfur source instead of Na_2S. Because of their low reactivity, the reaction temperatures were elevated to 100 °C. Figure S4, Supporting Information shows the TEM images of the products converted from spherical Cu_2O (Figure 2a). It shows that hollow spheres were obtained when thioacetamide was used, while irregular solid particles dominated the products with thiourea as a sulfur source. Since the S-releasing rate of the three type of sulfur sources follows the sequence of Na_2S > thioacetamide > thiourea, it can be concluded that the relative higher concentration of S^{2-} ions benefited the formation of hollow structures.

Although it is in common use to synthesize Cu_7S_4 nanocrystals with Cu_2O as sacrificial templates,[21] there are seldom reports on the fabrication of CuS via a similar process.[22] The presumed transformation mechanism from Cu_2O to Cu_xS is the dissolved-oxygen-assisted oxidation from Cu^+ to Cu^{2+} and the subsequent sulfidation. By comparison the reaction parameters for the production of CuS and Cu_7S_4, it can be concluded that the reaction parameters including the concentration of the reactants, the sulfur source, the reaction temperature, and duration times are all kept the same. The major difference is the remains of NaOH, PVP, and Vc in the reaction solution for the fabrication of Cu_7S_4 and the separation-drying process of Cu_2O templates for the fabrication of CuS. To address the roles of the remains, we performed the control experiments by keeping all other conditions the same as those for the fabrication of CuS but with the additional introduction of NaOH, PVP, or Vc, respectively. Definitely, after being separated and dried, the as-prepared Cu_2O nanotemplates were dispersed into 40.0 mL of glycol, upon which given amounts of NaOH, PVP, or Vc were introduced, respectively. Then, 20.0 mL of Na_2S (0.15 mol·L^{-1}) glycol solution was added into the mixture and the reaction was kept at 55 °C for 1 h. As discussed in the previous works,[19] PVP mainly functions as the structure-directing agent for the construction of Cu_2O nanospheres and thus were not consumed during the reaction, while Vc and NaOH were all involved in the chemistry reaction in the formation of Cu_2O. Considering the consumption amounts of Vc and NaOH are not very concrete, we adopted two extreme values (the initial introducing amounts and the remaining amounts assuming the complete conversion from Cu^{2+} to Cu_2O) for investigation. The detailed description can be seen in Supporting Information. XRD characterizations demonstrate that all the products can be identified as CuS as shown in Figure S5. It reveals that the remains in the solution were not the primary parameters affecting the stoichiometry of the products.

To learn more information, we carried out the FTIR and XPS characterizations on the separated Cu_2O nanocrystals. XPS is a powerful technique for surface analysis, especially for the detection of variation in the oxidation state. Copper exists in a monovalent state with full 3d shell in Cu_2O, while it exhibits a divalent state with d^9 character in CuO. The XPS spectrum (Figure 4a) displays two strong peaks located at around 932.1 and 951.9 eV, which can be assigned to Cu $2p_{3/2}$ and Cu $2p_{1/2}$ of Cu^+, respectively.[23] Besides these two main peaks, a series of satellites are observed at the high energy sides such as 944.0, 946.2, 954.8, and 962.3 eV. It is generally accepted that these

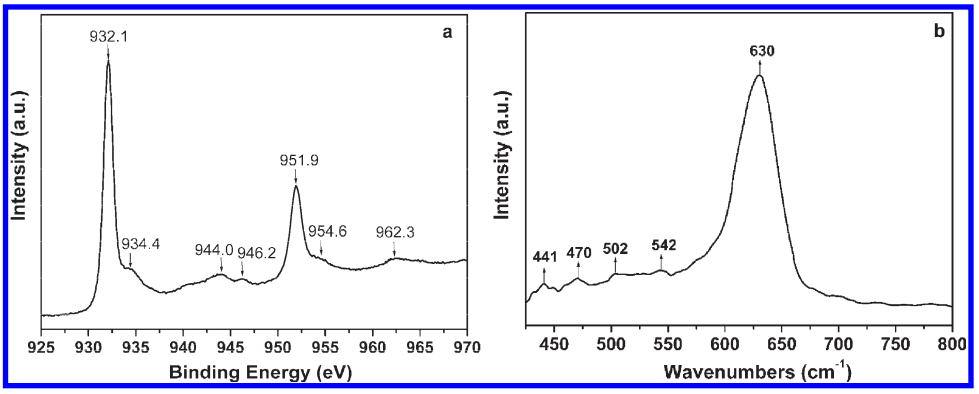

Figure 4. (a) Detailed core level XPS spectra of copper (2p) and (b) FTIR spectra of the Cu_2O after being separated and dried.

shakeup features are the characteristics of Cu^{2+} in CuO.[24] Therefore, the XPS results demonstrate that the Cu_2O nanocrystals were partially oxidized into CuO during the washing and drying processes. The relative weak intensities of the satellites indicate the small fracture of the CuO. FTIR measurements provide additional evidence for the existence of CuO. As shown in Figure 4b, the strong absorption peak located at around 630 cm^{-1} is the characteristic vibration of Cu(I)-O, while the four relatively weak but obvious vibrations at around 544, 502, 470, and 441 cm^{-1} are believed to be contributed from the Cu(II)-O vibrations.[25] Combined with the fact of no diffractions from CuO detected in the XRD pattern, it can be concluded that only a small degree of Cu_2O was oxidized and the formed CuO might be amorphous.

Kirkendall-based process was believed to be responsible for the transformation from Cu_2O to Cu_xS hollow structures. When Na_2S was introduced into the Cu_2O-containing mother solution, the extremely small K_{sp} of copper sulfide ($\approx 1.0 \times 10^{-48}$, 298 K) promoted the sulfidation process. The partially oxidization of the Cu^+ by the dissolved oxygen allowed Cu_7S_4 rather than Cu_2S nanocrystals to be produced. The formed thin layer of Cu_7S_4 acted as the interface for the next reaction. Since the diffusion rate of sulfur ions from the surface to the inner part was considerably slower than that of Cu anions from the inner part to the surface, hollow structures with enlarged inner voids resulted, which is a typical character of the Kirkendall process.[17,21,26] To trace the transformation process, the reaction was stopped 5 min later after Na_2S was added. The intermediates were collected by centrifugation and washed several times with ethanol and distilled water. The corresponding XRD pattern can be indexed to the superimposition of the cuprite Cu_2O (as denoted with star) and monoclinic Cu_7S_4 (as marked with squares) as shown in Figure 5a. TEM observations demonstrate the intermediates exhibited as core−shell structures. Figure 5b is a typical TEM image for such a core−shell structure. The corresponding HRTEM characterization (Figure 5c) further confirmed the composition profile. The observed lattice spacing of 0.24 nm in the core corresponds to the (111) plane of the cuprite Cu_2O. The measured spacings are 0.18 and 0.30 nm in the shell, agreeing well with the (886) and (804) facets of Cu_7S_4, respectively.

When the Cu_2O nanocrystals were separated and dried, thin layers of CuO must have covered the outsides of the Cu_2O nanocrystals as evidenced by the XPS and FTIR characterizations, which might be facilitated by the adsorbed water and the oxygen in air. In fact, several reports have demonstrated the easy

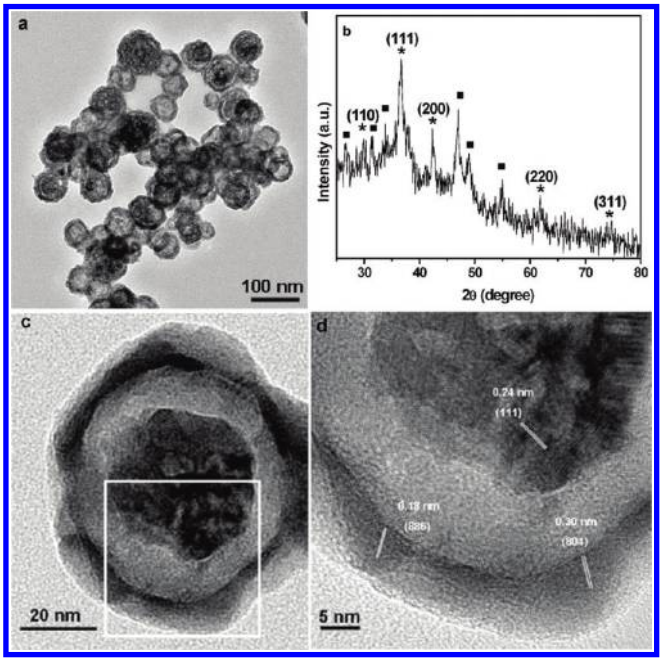

Figure 5. The morphology and structure of the intermediates of sample A. (a) Survey TEM images, (b) XRD pattern, (c) high-magnification TEM image, and (d) HRTEM image recorded in the framed box as indicated in (c).

oxidation of Cu_2O nanocrystallites into CuO.[22b,23b] According to the experimental conditions, the concentration of S^{2-} is about 0.046 mol·L^{-1}. On the basis of the fact that K_{sp}(CuS) is 6.3×10^{-36} and $K_{sp}(Cu_2S)$ is 1.0×10^{-48}, it can be calculated that to form the corresponding sulfides, the concentration of Cu^{2+} should be at least 1.6×10^{-34} while that of Cu^+ is about 5.0×10^{-24}. That is, under the same concentration of S^{2-}, CuS is the first to form, which resulted in the conversion from CuO to CuS. However, how does such a thin layer of CuO allow the Cu_2O-dominated nanocrystals to transform entirely into CuS rather than a mixture of CuS and Cu_7S_4?

Taking into account the production of Cu_7S_4 with untreated Cu_2O as templates, we believed that CuO had served as a catalysis for the oxidation from Cu^+ to Cu^{2+}. In fact, copper-based catalysts have been widely used in chemical and biomolecules synthesis.[27] Suib's work demonstrated that urchin-like CuO nanocrystals are effective catalysts to improve the yield for olefin epoxidation.[28] Kantam et al. reported that nanocrystalline CuO

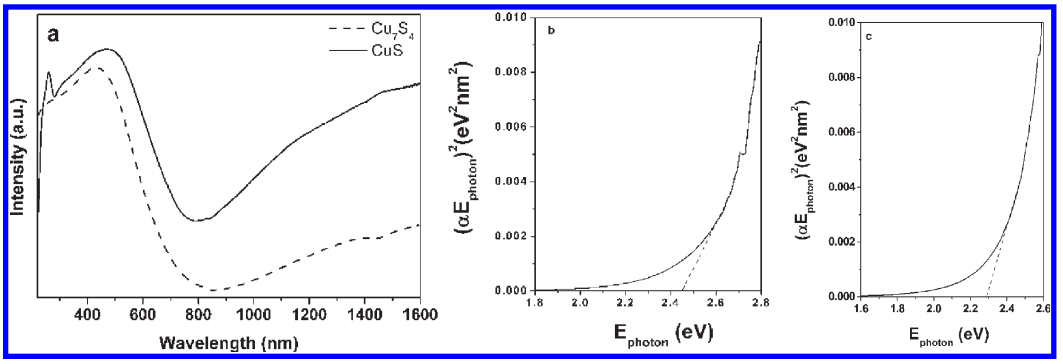

Figure 6. (a) UV−vis−NIR spectra, and (b, c) $(\alpha E_{photon})^2/E_{photon}$ plots of Cu_7S_4 and CuS hollow nanospheres, respectively.

exhibits excellent catalytic activities for CO and NO oxidation.[29] In addition, C−N, C−S coupling reactions also were reported using CuO as a catalysis.[30] It is rational that during the diffusion of Cu^+ ions from the inner part to the surface, the CuO covering the outlayer of Cu_2O catalyzed the oxidation from Cu^+ to Cu^{2+} in the presence of the dissolved oxygen. In conjunction with the fact that the XRD pattern of the intermediates of sample B (Figure S2, Supporting Information) can be indexed to the mixture of Cu_2O and CuS, it can be concluded that the Cu_2O was gradually oxidized and the sulfidation occurred instantly after the Cu^{2+} was produced.

It is well-known that the Cu^+ ions in solution transform into Cu^{2+} and Cu through a dismutation reaction following eq 1.

$$2Cu^+ \rightleftharpoons Cu^{2+} + Cu \quad (1)$$

The precipitation of CuS would promote the balance shift toward the formation of Cu^{2+}, which is one possible reason for the thorough oxidation. However, no signal from Cu detected in the final product excluded this possibility.

A prominent feature for copper sulfides is the varied band gaps and structures with varying stoichiometries. Stimulated by the rich optical properties, we investigated the UV−vis−NIR absorption behaviors of the as-prepared copper sulfides, which formed steady suspension in ethanol facilitated by their thin-shell structures. As shown in Figure 6a, the spectrum of CuS displays two absorptions centered at around 260 and 464 nm. The latter one is consisent with the reported data for CuS hollow spheres fabricated in different methods.[31,32] As for the sharp shoulder at around 260 nm, it was similar to the weak adsorptions at ~310 nm as observed in the previous reports.[33−35] Although its origin is still ambiguous, we believe it is contributed from the quantum confinement effect of the primary nanoparticles assembled into hollow spheres as revealed in SEM and TEM observations. Besides these two peaks, a strong absorption at near IR region is also observed, which is accepted as the characteristic of covellite (CuS).[36] The Cu_4S_7 hollow spheres exhibit a broad absorption centered at ~437 nm. Figure 6a also demonstrates that the near-IR absorption also appeared for Cu_7S_4 hollow spheres but with lower intensity compared with that for CuS. The NIR absorptions for copper sulfides are believed to derive from the free carriers. The stoichiometric-dependent feature observed in our case is coincident with the trends for bulk counterparts.[37] And similar observations were also reported in Burda's work for $Cu_{2-x}S$ nanocrystals synthesized with different methods.[18]

Their band gap energies were estimated according to a classical Tauc approach.[38] In the case of direct transition, $(\alpha E_{photon})^2$ versus E_{photon} was plotted, where $\alpha = \log(I^0/I)/(lc/\rho)$; I^0 and I are the intensities before and after transmission, respectively, l is the present path length, 10 mm, and ρ is the Cu_xS density, 0.0056 g/cm^3, c is the concentration of the suspension of the copper sulfide, which is estimated as 0.045 g/L. It should be mentioned that since the absorbance was obtained by measuring the transmission spectra of the Cu_xS suspension, the calculated value of α also includes the scattering and reflection loss in principle. However, since the suspension is transparent under such a low concentration, the scattering and reflection loss are generally ignored. The plots of Cu_7S_4 and CuS are shown in Figure 6, panels b and c, respectively. The extrapolated value of E_{photon} at $\alpha = 0$ gives an absorption edge energy corresponding to E_{gap} = 2.44 eV for Cu_7S_4 and 2.31 eV for CuS hollow spheres. In comparison with the data of values of 1.2 eV[39] and 1.34 eV[40] for their bulk counterparts, it is reasonable to conclude that a considerable blue shift has occurred. It presumably resulted from the quantum size effects considering the polycrystalline feature of the hollow spheres.

CONCLUSIONS

Copper sulfides hollow structures with controlled stoichiometries, Cu_7S_4 and CuS, were achieved by in situ transformation of Cu_2O nanocrystals with different surface states. The direct introduction of S^{2-} glycol solution into the Cu_2O-containing mother solution produced Cu_7S_4 nanocrystals, while CuS formed with Cu_2O experienced a separation and drying process as sacrificial templates. The presence of CuO, as evidenced by XPS and FTIR data, is believed to catalyze the oxidation from Cu^+ to Cu^{2+}. A Kirkendall-based process was proposed to illustrate the transformation. The sulfur source was found have an important impact on the morphologies of the products. Significant quantum confinement effect and stoichiometric-dependent features were demonstrated in the UV−vis−NIR absorption investigations.

ASSOCIATED CONTENT

Supporting Information. The broad view SEM images of Cu_2O, Cu_7S_4, and CuS hollow spheres, XRD pattern of the intermediates during the transformation from Cu_2O to CuS, the SEM, TEM images, and XRD patterns of the products with Cu_2O octadrons as templates, the XRD patterns of the products of control experiments. TEM images of the products with thioacetamide and thiourea as sulfur sources. This material is available free of charge via the Internet at http://pubs.acs.org.

AUTHOR INFORMATION

Corresponding Author
*Phone: +86-10-82338162; e-mail: guolin@buaa.edu.cn.

ACKNOWLEDGMENT

The authors are thankful for the financial support from National Basic Research Program of China (No. 2010-CB934700), National Nature Science Foundation of China (20803002, 20973019 & 50725208), Research Fund for the Doctoral Program of Higher Education of China (No 2007-0006016), and Weishi research Fund of Beihang (YWF-11-03-Q-085).

REFERENCES

(1) Galdikas, A.; Mironas, A.; Strazdiene, V.; Setkus, A.; Ancutiene, I.; Janichis, V. *Sens. Actuators B* **2000**, *67*, 76.
(2) Setkus, A.; Galdikas, A.; Mironas, A.; Simkiene, I.; Ancutiene, I.; Janichis, V.; Kaciulis, S.; Mattogno, G.; Ingo, G. M. *Thin Solid Films* **2001**, *391*, 275.
(3) Mulder, B. J. *Phys. Status Solidi A* **1972**, *13*, 79.
(4) Reijnen, L.; Meester, B.; Goossens, A.; Schoonman, J. *Chem. Vap. Deposition* **2003**, *9*, 15.
(5) Nascu, C.; Pop, I.; Ionescu, V.; Indrea, E.; Bratu, I. *Mater. Lett.* **1997**, *32*, 73.
(6) Sagade, A. A.; Sharma, R. *Sens. Actuators, B* **2008**, *133*, 135.
(7) (a) Kalyanikutty, K. P.; Nikhila, M.; Maitra, U.; Rao, C. N. R. *Chem. Phys. Lett.* **2006**, *432*, 190. (b) Roy, P.; Srivastava, S. K. *Mater. Lett.* **2007**, *61*, 1693. (c) Larsen, T. H.; Sigman, M.; Ghezelbash, A.; Doty, R. C.; Korgel, B. A. *J. Am. Chem. Soc.* **2003**, *125*, 5638. (d) Sigman, M. B.; Ghezelbash, A.; Hanrath, T.; Saunders, A. E.; Lee, F.; Korgel, B. A. *J. Am. Chem. Soc.* **2003**, *125*, 16050. (e) Roy, P.; Mondal, K.; Srivastava, S. K. *Cryst. Growth Design* **2008**, *8*, 1530.
(8) Wu, C. Y.; Yu, S. H.; Chen, S. F.; Liu, G. N.; Liu, B. H. *J. Mater. Chem.* **2006**, *16*, 3326.
(9) (a) Fang, Z.; Wang, X. Y.; Shen, J. M.; Lin, X.; Ni, Y. H.; Wei, X. W. *Cryst. Growth Des.* **2010**, *10*, 469. (b) Zhang, H. T.; Wu, G.; Chen, X. H. *Mater. Chem. Phys.* **2006**, *98*, 298.
(10) Feng, X. P.; Li, Y. X.; Liu, H. B.; Li, Y. L.; Cui, S.; Wang, N.; Jiang, L.; Liu, X. F.; Yuan, M. J. *Nanotechnology* **2007**, *18*, 145706.
(11) Lai, C. X.; Wu, Q. B.; Chen, J.; Wen, L. S.; Ren, S. *Nanotechnology* **2010**, *21*, 215602.
(12) Xu, H. L.; Wang, W. Z.; Zhu, W.; Zhou, L. *Nanotechnology* **2006**, *17*, 3649.
(13) (a) Zhu, H.; Ji, X.; Yang, D.; Ji, Y.; Zhang, H. *Microporous Mesoporous Mater.* **2005**, *80*, 153. (b) Ni, Y.; Liu, H.; Wang, F.; Yin, G.; Hong, J.; Ma, X.; Xu, Z. *Appl. Phys. A: Mater. Sci. Process.* **2004**, *79*, 2007. (c) Gao, J. N.; Li, Q. S.; Zhao, H. B.; Li, L. S.; Liu, C. L.; Gong, Q. H.; Qi, L. M. *Chem. Mater.* **2008**, *20*, 6263. (d) Ge, L.; Jing, X. Y.; Wang, J.; Jamil, S.; Liu, Q.; Song, D. L.; Wang, J.; Xie, Y.; Yang, P. P.; Zhang, M. L. *Cryst. Growth Des.* **2010**, *10*, 1688.
(14) (a) Lou, Y. B.; Samia, A. C. S.; Cowen, J.; Banger, K.; Chen, X. B.; Lee, H.; Burda, C. *Phys. Chem. Chem. Phys.* **2003**, *5*, 1091. (b) Larsen, T. H.; Sigman, M.; Ghezelbash, A.; Doty, R. C.; Korgel, B. A. *J. Am. Chem. Soc.* **2003**, *125*, 5638.
(15) Yu, X. L.; Cao, C. B.; Zhu, H.; Li, Q. S.; Liu, C. L.; Gong, Q. H. *Adv. Funct. Mater.* **2007**, *17*, 1397.
(16) (a) Cao, H. L.; Qian, X. F.; Wang, C.; Ma, X. D.; Yin, J.; Zhu, Z. K. *J. Am. Chem. Soc.* **2005**, *127*, 16024. (b) Xu, J.; Zhang, W. X.; Yang, Z. H.; Yang, S. H. *Inorg. Chem.* **2008**, *47*, 699.
(17) Jiao, S. H.; Xu, L. F.; Jiang, K.; Xu, D. S. *Adv. Mater.* **2006**, *18*, 1174.
(18) Zhao, Y. X.; Pan, H. C.; Lou, Y. B.; Qiu, X. F.; Zhu, J. J.; Burda, C. *J. Am. Chem. Soc.* **2009**, *131*, 4253.
(19) Zhang, H.; Zhang, D. F.; Guo, L.; Zhang, R.; Yin, P. G.; Wang, R. M. *J. Nanosci. Nanotechnology* **2008**, *8*, 6332.
(20) Zhang, D. F.; Zhang, H.; Guo, L.; Zheng, K.; Han, X. D.; Zhang, Z. *J. Mater. Chem.* **2009**, *19*, 5220.
(21) (a) Cao, H. L.; Qian, X. F.; Wang, C.; Ma, X. D.; Yin, J.; Zhu, Z. K. *J. Am. Chem. Soc.* **2005**, *127*, 16024. (b) Zhang, W. X.; Xu, J.; Yang, Z. H.; Ding, S. X. *Chem. Phys. Lett.* **2007**, *434*, 256. (c) Zhang, W. X.; Chen, Z. X.; Yang, Z. H. *Phys. Chem. Chem. Phys.* **2009**, *11*, 6263.
(22) (a) Zhu, H. T.; Wang, J. X.; Wu, D. X. *Inorg. Chem.* **2009**, *48*, 7099. (b) Pang, M. L.; Zeng, H. C. *Langmuir* **2010**, *26*, 5963.
(23) (a) Midander, K.; Cronholm, P.; Karlsson, H. L.; Elihn, K.; Möller, L.; Leygraf, C.; Wallinder, I. O. *Small* **2009**, *5*, 389. (b) Yin, M.; Wu, C. K.; Lou, Y. B.; Burda, C.; Koberstein, J. T.; Zhu, Y. M.; O'Brien, S. *J. Am. Chem. Soc.* **2005**, *127*, 9506. (c) Ghijsen, J.; Tjeng, L. H.; Elp, J. v.; Eskes, H.; Westerink, J.; Sawatzky, G. A. *Phys. Rev. B* **1988**, *38*, 11322.
(24) (a) Yin, M.; Wu, C. K.; Lou, Y. B.; Burda, C.; Koberstein, J. T.; Zhu, Y. M.; O'Brien, S. *J. Am. Chem. Soc.* **2005**, *127*, 9506. (b) Chusuei, C. C.; Brookshier, M. A.; Goodman, D. W. *Langmuir* **1999**, *15*, 2806. (c) Jagminas, A.; Kuzmarskyté, J.; Niaura, G. *Appl. Surf. Sci.* **2002**, *201*, 129.
(25) (a) Kliche, G.; Popovic, Z. V. *Phys. Rev. B: Condens. Matter. Mater. Phys.* **1990**, *42*, 10060. (b) Narang, S. H.; Kartha, V. B.; Patel, N. D. *Physica C* **1992**, *204*, 8.
(26) (a) Yin, Y. D.; Rioux, R. M.; Erdonmez, C. K.; Hughes, S.; Somorjai, G. A.; Alivisatos, A. P. *Science* **2004**, *30*, 711. (b) Fan, H. J.; Gçsele, U.; Zacharias, M. *Small* **2007**, *3*, 1660and the references therein.
(27) Evano, G.; Blanchard, N.; Toumi, M. *Chem. Rev.* **2008**, *108*, 3054.
(28) Xu, L. P.; Sithambaram, S.; Zhang, Y.; Chen, C. H.; Jin, L.; Joesten, R.; Suib, S. L. *Chem. Mater.* **2009**, *21*, 1253.
(29) Liu, Y.; Fu, Q.; Stephanopoulos, M, F. *Catal. Today* **2004**, *93*−*95*, 241.
(30) (a) Kantam, M. L.; Yadav, J.; Laha, S.; Sreedhar, B.; Jha, S. *Adv. Synth. Catal.* **2007**, *349*, 1938. (b) Jammi, S.; Sakthivel, S.; Rout, L.; Mukherjee, T.; Mandal, S.; Mitra, R.; Punniyamurthy, T. *J. Org. Chem.* **2009**, *74*, 1971.
(31) Yu, X.; Cao, C.; Zhu, H.; Li, Q.; Liu, C.; Gong, Q. *Adv. Funct. Mater.* **2007**, *17*, 1397.
(32) Gao, J. N.; Li, Q. S.; Zhao, H. B.; Li, L. S.; Liu, C. L.; Gong, Q. H.; Qi, L. M. *Chem. Mater.* **2008**, *20*, 6263.
(33) Liu, J.; Xue, D. F. *J. Cryst. Growth* **2009**, *311*, 500.
(34) Li, F.; Bi, W. T.; Kong, T.; Qin, Q. H. *Cryst. Res. Technol.* **2009**, *44*, 729.
(35) Xu, H. L.; Wang, W. Z.; Zhu, W. *Mater. Lett.* **2006**, *60*, 2203.
(36) Haram, S. K.; Mahadeshwar, A. R.; Dixit, S. G. *J. Phys. Chem.* **1996**, *100*, 5868.
(37) Dixit, S. G.; Mahadeshwar, A. R.; Haram, S. K. *Colloids Surf., A* **1998**, *133*, 69.
(38) Tsunekawa, S.; Fukuda, T.; Kasuya, A. *J. Appl. Phys.* **2000**, *87*, 1318.
(39) Marshall, R.; Mitra, S. S. *J. Appl. Phys.* **1965**, *36*, 3882.
(40) Haram, S. K.; Mahadeshwar, A. R.; Dixit, S. G. *J. Phys. Chem.* **1996**, *100*, 5868.